Anomalous temperature-dependent heat transport in one-dimensional momentum-conserving systems with soft-type interparticle interaction

Daxing Xiong*
Department of Physics, Fuzhou University, Fuzhou 350108, Fujian, China
(Received 12 December 2016; published 19 April 2017)

We numerically investigate the heat transport problem in a one-dimensional momentum-conserving lattice with a soft-type (ST) anharmonic interparticle interaction. It is found that with the increase of the system's temperature, while the introduction of ST anharmonicity softens phonons and decreases their velocities, this type of nonlinearity like its hard type (HT) counterpart, can still not be able to fully damp the longest wavelength phonons. Therefore, a usual anomalous temperature dependence of heat transport with certain scaling properties similarly to those shown in the Fermi-Pasta-Ulam-β-like systems with HT interactions can be seen. Our detailed examination from simulations verifies this temperature-dependent behavior well.

DOI: 10.1103/PhysRevE.95.042127

I. INTRODUCTION

As one of the fundamental topics closely related to the concepts of nonlinearity and irreversibility in statistical mechanics [1], heat transport in one-dimensional (1D) systems has attracted considerable interest in recent years [2–5]. In this context, one of the central issues is the validity or breakdown of Fourier's law, a celebrated empirical law for describing heat conduction stating that the heat flux J is proportional to the temperature gradient ∇T: $J = -\kappa \nabla T$, with κ the heat conductivity assumed to be a size-independent constant. Generally, now it has been well accepted that for 1D anharmonic systems with conserved momentum, Fourier's law is not valid, namely, κ is not a constant but diverges with the system size L in a power law $\kappa \sim L^{\alpha}$ [2,3,6–12]. The exponent α $(0 \leqslant \alpha \leqslant 1)$ is believed to following some universality classes [2,3,8–10,12–17]. Such universality classes have been supported by some theories [9,10,13–17] and numerical simulations [8,12,18,19] and debated by some other studies [20–26]. While it should be noted that if some other factors, such as the asymmetric interactions [27–31], the systems close to the integrable limit [32], the pressure [33,34], and the multiwell interparticle potential [35–41], are taken into account, whether the Fourier's law is still valid or not, and what the underlying mechanics are behind them, the verification remains in progress.

It is thus desirable to check the heat transport law including more complicated factors to seek general conclusions. In the present work we therefore consider a momentum-conserving system with the soft-type (ST) interparticle interaction, which we stress that is a factor that has not yet been fully taken into account [compared with the hard-type (HT) interactions]. Our main finding is that, similarly to the Fermi-Pasta-Ulam-β (FPU-β) systems with HT anharmonicity, a non-Fourier anomalous heat transport will be observed under all temperatures. Via detailed simulations we also explore the possible microscopic mechanisms. We show that with the increase of the system's temperature, the ST interaction induces a special type of nonlinearity, which softens phonons and reduces their velocities, while these unusual effects are still unable to qualitatively change the heat transport and its scaling property. A careful analysis of system's momentum spread and phonons spectrum indicates an incomplete damping process of phonons very similar to those exhibited in the FPU-β systems with HT anharmonicity. We conjecture that this may be the main mechanism for such a kind of anomalous temperature variation of heat transport observed here.

The remainder of this paper is organized as follows: In Sec. II we shall introduce the model with ST anharmonic interaction and compare it with the potentials of harmonic and FPU-β systems (with HT interactions). Section III will describe the simulation method. We shall use the equilibrium correlation simulation method [42,43] to derive the heat spreading information, from which our main results of heat transport and its scaling property are presented in Sec. IV. Section V is devoted to understanding the underlying mechanisms. For such a purpose we shall investigate the system's momentum spread and examine the phonons spectrum to explore phonons' damping information. Finally, a summary will be presented in the last section.

II. MODEL

The model we consider is a 1D many-particle (L particles) momentum-conserving lattice with Hamiltonian

$$H = \sum_{k=1}^{L} p_k^2/2 + V(r_{k+1} - r_k). \tag{1}$$

In this Hamiltonian p_k is the kth particle's momentum and r_k is its displacement from an equilibrium position. The interparticle potential takes a type of soft anharmonicity [44–46]

$$V(\xi) = |\xi| - \ln(1 + |\xi|). \tag{2}$$

For such a system, we set the averaged distance between particles and the lattice constant to be unity; thus the number of particles is identical to the system size L.

In Fig. 1(a) we plot this ST anharmonic potential and compare it with the harmonic [$V(\xi) = \xi^2/2$] and FPU-β [$V(\xi) = \xi^2/2 + \xi^4/4$] potentials. Figure 1(b) further presents their associated forces defined by $F(\xi) = -\partial V(\xi)/\partial \xi$. As can be seen, unlike the FPU-β system with HT anharmonicity, the ST

*phyxiongdx@fzu.edu.cn

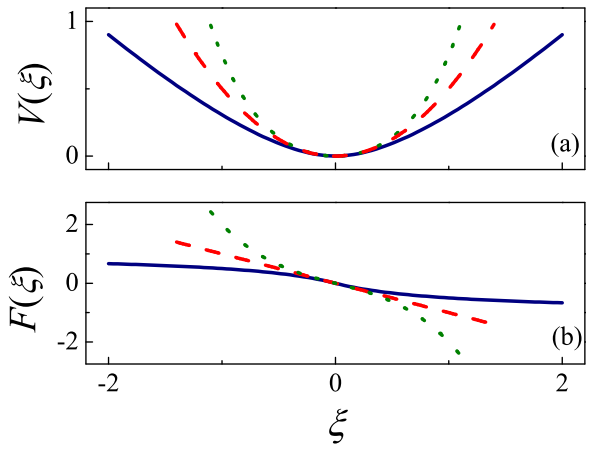

FIG. 1. The ST anharmonic interparticle potential [Eq. (2), solid] (a) and its associated force (b). For comparison we also plot the cases of the harmonic (dashed) and FPU-β (dotted) systems.

interaction has a restoring force always less than the harmonic force. This is why we call it ST anharmonicity, a special feature of the system. It induces an unusual energy-dependent frequency [44], which has been suggested to strongly modify the distribution, intensity, and mobility of the thermal fluctuations, resulting in a quite different transition dynamics of the underlying activated process [46]. In the research field of discrete breathers (DBs), such ST anharmonicity can also support a different amplitude-dependent property of DBs' frequency, opposite to that induced by HT anharmoncity [47]. Motivated by this microscopic evidence, we here aim to explore how such ST anharmonicity would play roles in heat transport.

III. METHOD

As mentioned, to identify the heat transport property and its scaling behavior, we use the equilibrium correlation simulation method [42,43]. For the special ST anharmonicity, it could be expected that the time scale ensuring the system relaxed to the nonequilibrium stationary state would be much longer than the usual considered FPU-β systems with HT anharmonicity. This would be why the traditional simulation methods, such as the direct nonequilibrium molecular dynamics simulations [7] and the approach based on the Green-Kubo formula to explore the heat flux correlation [9], have not yet been adopted to study such a system, and thus the heat transport law here is still unclear.

Compared with the traditional methods [7,9], the equilibrium correlation method [42,43] employs the following normalized spatiotemporal correlation function of system's heat energy fluctuations to explore the heat spreading information:

$$\rho_Q(m,t) = \frac{\langle \Delta Q_j(t) \Delta Q_i(0) \rangle}{\langle \Delta Q_i(0) \Delta Q_i(0) \rangle}, \tag{3}$$

where $m = j - i$; $\langle \cdot \rangle$ represents the spatiotemporal average; i and j denote the labels of bins; this is because in hydrodynamics theory, the heat energy density should be defined as a function of space rather than the lattice site. Viewing this fact, we set the number of particles in the ith bin to be $N_i = L/b$, where b is the total number of the bins. Under this setup, in each bin one can compute the energy $E_i(t)$, particle $M_i(t)$, and pressure $F_i(t)$ densities by summing the corresponding single particles' densities $E(k,t)$, $M(k,t)$, and $F(k,t)$ at the site k and time t within the bin. The heat energy density in the ith bin then is $Q_i(t) \equiv E_i(t) - \frac{(\langle E \rangle + \langle F \rangle) M_i(t)}{\langle M \rangle}$ [48,49], and its fluctuation $\Delta Q_i(t) \equiv Q_i(t) - \langle Q_i \rangle$ can be straightforwardly obtained. From this definition we know that heat energy in one bin is closely related to the associated energy and particle densities under an internal averaged pressure $\langle F \rangle$ ($\equiv 0$, since the potential here is symmetric and the averaged distance between particles is identical to the lattice constant).

In order to provide additional information for the underlying physics, we also study the momentum spread via the momentum correlation function

$$\rho_p(m,t) = \frac{\langle \Delta p_j(t) \Delta p_i(0) \rangle}{\langle \Delta p_i(0) \Delta p_i(0) \rangle}. \tag{4}$$

Similarly to the definition of $\rho_Q(m,t)$, here $\Delta p_i(t) \equiv p_i(t) - \langle p_i \rangle$ denotes the momentum fluctuation in the ith bin.

To calculate both correlation functions, the system is first thermalized to the focused temperature by using the stochastic Langevin heat baths [2,3] for a long enough time ($>10^7$ time units of the model). This should be done from properly assigned initial random states. Then the system is evolved in isolation by using the Runge-Kutta algorithm on seventh to eighth order with a time step h for deriving the correlation information. We use an ensemble size about 8×10^9.

We consider a wide range of temperatures from $T = 0.00075$ to $T = 1$. For each temperature, we set $L = 2001$, which will allow the fluctuation of heat located at the center to spread along the system for a long time at least up to $t = 600 - 900$. Under this setup, we apply the periodic boundary conditions and fix the bin's number $b \equiv 1000$ (the choice of b has been verified not to affect the final results).

The difficulty in simulating the correlation functions for the ST anharmonic systems lies in the case of high temperatures. This is because due to the effect of phonons softening (shown below), a higher T will take us more time for simulations to ensure the system relaxed to the stationary state and will require a higher precision of integration with a much smaller time step h. Such calculations will cost many computing resources. Therefore, the highest temperature considered is $T = 1$ and for different temperatures different time steps h are used, i.e., for low temperatures, $h = 0.05$ is always adopted, while for the temperatures higher than $T = 0.5$, we set $h = 0.02$, which has been verified to be efficient for the system to evolve under satisfactory precision.

IV. HEAT SPREAD AND ITS SCALING

Figure 2 presents the profiles of $\rho_Q(m,t)$ for three typical times. Here the results of time up to $t = 600$ are used as examples. We do not present the longer time's results here because we have found the fact that this will cause the side peaks hard to detect in the high-temperature regimes [see Fig. 2(d)]. In addition, to show the temperature-dependent behavior, the results of four temperatures T, from low to high, are employed. As can be seen, with the increase of T, the profiles of $\rho_Q(m,t)$ are changed from a U-shaped [50] to a

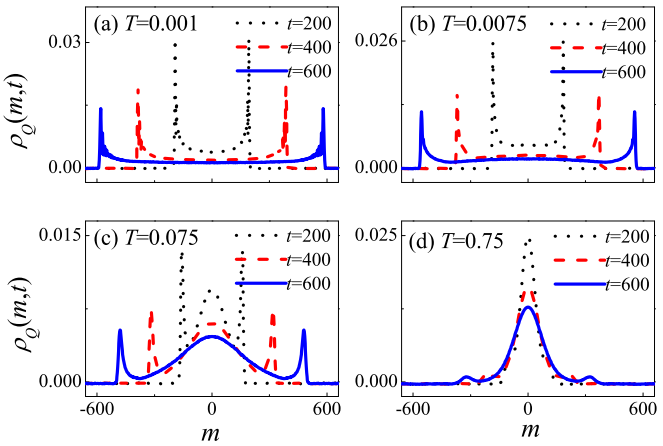

FIG. 2. Profiles of $\rho_Q(m,t)$ for three long times $t = 200$ (dotted), $t = 400$ (dashed), and $t = 600$ (solid) under temperatures $T = 0.001$ (a), $T = 0.0075$ (b), $T = 0.075$ (c), and $T = 0.75$ (d), respectively.

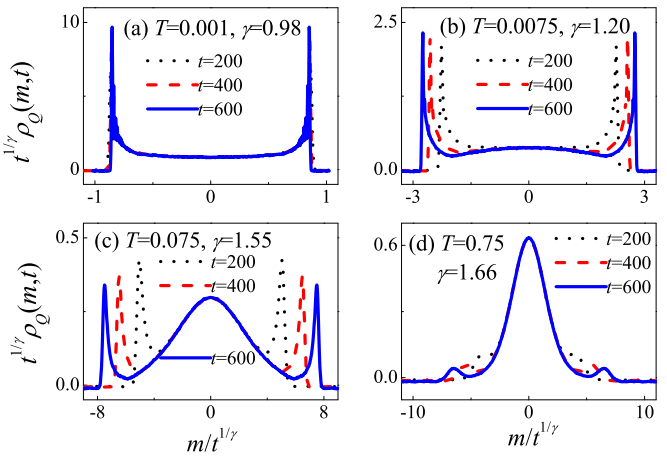

FIG. 3. Rescaled $\rho_Q(m,t)$, the focused temperatures here are the same as those in Fig. 2.

Lévy walk [15,16] density, especially where the central parts of the profiles become more and more localized. The U-shaped density shown here is slightly different from the usual density in a harmonic chain [50]; i.e., the front parts exhibit some oscillations, which may be induced by the unusual nonlinearity of the ST anharmonicity under low temperatures. The Lévy walk profiles under high temperatures can be phenomenologically understood from the single particle's Lévy walk model in the superdiffusive regime after considering the velocity fluctuations [51].

In view of the coincidence with the Lévy walk profiles, one then can perform a scaling analysis to $\rho_Q(m,t)$ by using the following scaling formula [15,16]:

$$t^{1/\gamma}\rho_Q(m,t) \simeq \rho_Q\left(\frac{m}{t^{1/\gamma}},t\right). \tag{5}$$

Note that this scaling law applies to the central parts only if the underlying diffusion process is superdiffusive ($1 < \gamma < 2$), while for the ballistic ($\gamma = 1$) and normal diffusive ($\gamma = 2$) transport, it is valid for all of the ranges of density [15,16]. For the formula applying to high dimensions, one can refer to recent work on two-dimensional Lévy walks [52]. The rescaled profiles under formula (5) are shown in Fig. 3. This scaling property then enables us to identify a space-time scaling exponent γ for precisely characterizing the heat spreading behavior. Since $\gamma = 1$ and $1 < \gamma < 2$ correspond to the ballistic and superdiffusive heat transport, respectively, now we can understand that the U shape shown at low temperatures [$\gamma = 0.98$ close to 1, see Fig. 3(a)] indicates the ballistic heat transport, while the Lévy walk density under high temperatures implies the superdiffusive behavior [Fig. 3(d), $\gamma = 1.66 > 1$]. For the ballistic regime the whole density can be perfectly scaled by formula (5), for both the central and front parts, while in the superdiffusive regime, only the central parts are available, which might correspond to the bilinear scaling property of Lévy walks model in the superdiffusive regime [53,54].

To further demonstrate such bilinear scaling property, following Refs. [53,54], we use $\rho_Q(m,t)$ to calculate the q ($q > 0$) order momentum, i.e., $\langle|m(t)|^q\rangle = \int_{-\infty}^{\infty} |m(t)|^q \rho_Q(m,t)\, dm$, which for a strong anomalous diffusion process has been conjectured to satisfy $\langle|m(t)|^q\rangle \sim t^{q\nu(q)}$ with $\nu(q)$ not a constant [55]. For the specific Lévy walk model with $1 < \gamma < 2$ (γ here is the power law exponent from the waiting time distribution $\phi(\tau) \sim \tau^{-1-\gamma}$ of the model; see Refs. [53,54] for details), it has been predicted that for the low order q, $\langle|m(t)|^q\rangle \sim t^{q/\gamma}$, while for high order q, $q\nu(q) = q + 1 - \gamma$ [53,54]. As an example, the result of $q\nu(q)$ versus q for the heat spread under $T = 0.75$ is plotted in Fig. 4, from which a bilinear scaling property can indeed be identified. Here the fitting value for the low order q is $\nu(q) \simeq 0.63$, coincident with the prediction of $1/\gamma \simeq 0.60$ [$\gamma = 1.66$ from Fig. 3(d)] according to the Lévy walk theory. Such a coincidence indicates that the dynamical scaling exponent γ considered here might correspond to the power law exponent of the waiting time distribution in the Lévy walk model.

Employing this scaling exponent γ to understand anomalous heat transport is of great interest. It has been conjectured that from the result of γ one might infer the time scaling behavior of the mean-squared deviation of this heat diffusion process and thus connected to the system-size–dependent divergence exponent α [56–58]. Due to this common interest,

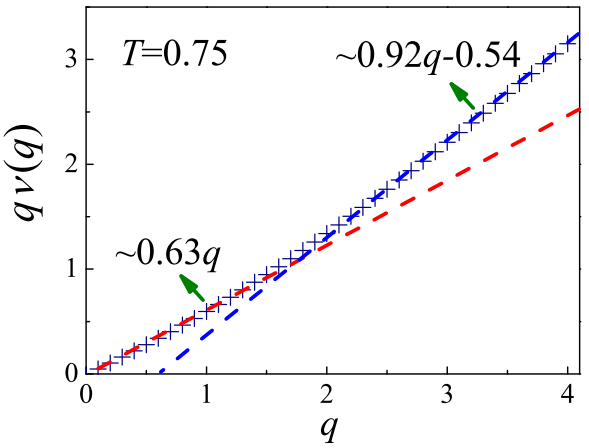

FIG. 4. Exponents $q\nu(q)$ vs q for indicating the bilinear scaling behavior. Here we take the case of $T = 0.75$ as an example.

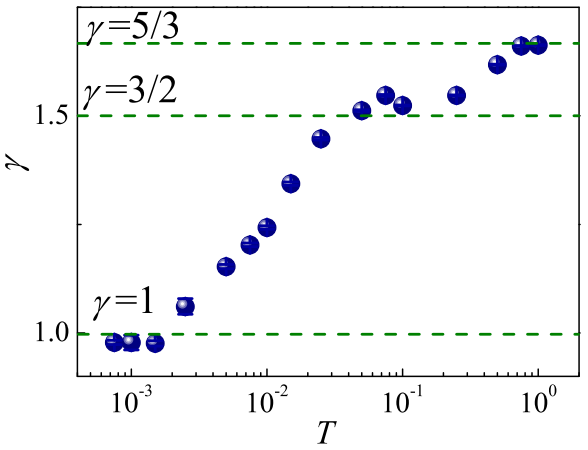

FIG. 5. γ vs T; the horizontal dashed lines, from bottom to top, denote $\gamma = 1$, $\gamma = 3/2$, and $\gamma = 5/3$, respectively.

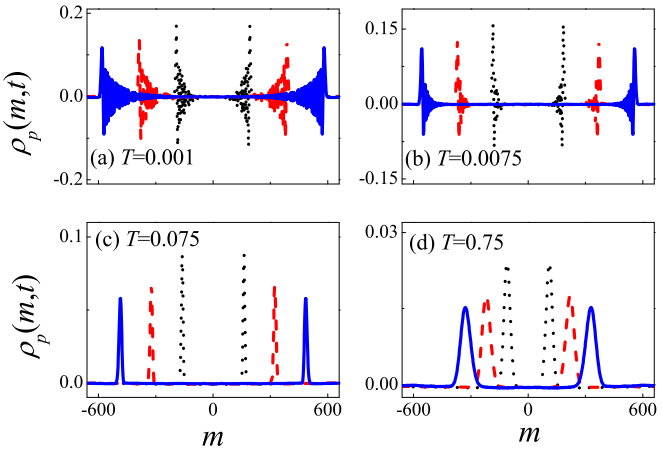

FIG. 6. Momentum spread $\rho_p(m,t)$ for three long time $t = 200$ (dotted), $t = 400$ (dashed), and $t = 600$ (solid) under temperatures $T = 0.001$ (a), $T = 0.0075$ (b), $T = 0.075$ (c), and $T = 0.75$ (d), respectively.

Fig. 5 further depicts the result of γ versus T. Therein four data points are extracted from Fig. 3, while others are obtained from the same scaling analysis. This result indicates that with the increase of T, γ first remains constant at about $\gamma \simeq 1$, then follows a temperature-dependent behavior in the intermediate range of T, and finally seems to saturate at $\gamma = 5/3$ for high temperatures. Interestingly, such a temperature variation of γ is similar to that shown in the FPU-β chains [40], where the nonlinearity dependence of γ values' crossover between different universality classes have been reported. As comparison to the related theories, we note that a recent understanding from hydrodynamics theory [14] suggested two universality classes of γ, $\gamma = 3/2$ and $\gamma = 5/3$, for the systems with symmetric and asymmetric interactions under zero and nonzero internal averaged pressure $\langle F\rangle$, respectively; however, for the special ST anharmonic system with symmetric potential and $\langle F\rangle = 0$ considered here, it seems that the prediction of $\gamma = 3/2$ is not always valid. In fact, such a nonuniversal scaling law has also been supported by some other theories [17,23–25] and numerical results [26].

V. UNDERLYING MECHANISM

Why does such anomalous temperature-dependent heat transport happen? Are there any new properties after including the ST anharmonic interaction? To provide insights into these issues, below we shall follow Ref. [41] to study both the momentum spread and the properties of phonons damping the system.

A. Momentum spread

The momentum spread contains useful information in understanding the heat transport of momentum-conserving systems. From the perspective of hydrodynamics theory, it may represent the diffusion of sound modes [43]. A recent work has attributed the observed normal heat transport in the coupled rotator systems to the diffusive behavior of momentum spread [60]. This nonballistic spread of momentum has also been found in a system with a double-well interparticle interaction under certain temperature ranges, where the normal heat transport can be observed [41]. For some integrable systems following ballistic heat transport, based on a new concept of phonon random walks, the ballistic momentum spread is proved to be a quantum like wave function's real part [50]. Therefore, ballistic (nonballistic) momentum spread always seems the case for anomalous (normal) heat transport.

Figure 6 depicts the results of momentum spread $\rho_p(m,t)$. Here, three long times and four typical temperatures the same as those in heat spread are considered. As can be seen, the results of the momentum spread also indicate interesting temperature-dependent evidences, i.e., while at low temperatures there are some oscillations in the profiles of $\rho_p(m,t)$ [see Fig. 6(a)]; with the increase of T, such oscillations become less and less [see Fig. 6(b)], and eventually disappear [see Fig. 6(c)]; after that if one increases T further, the front peaks begin to disperse [see Fig. 6(d)]. Thus, this unusual change of $\rho_p(m,t)$ with temperatures but still following ballistic transport may correspond to the anomalous temperature dependence of heat spread.

For the front peaks shown in $\rho_p(m,t)$, it has been suggested that its moving velocity just corresponds to the sound velocity c [59]. A recent theory [14] proposed a general formula

$$c = \sqrt{\frac{\frac{1}{2}T^2 + \langle V + \langle F\rangle\xi; V + \langle F\rangle\xi\rangle}{\frac{1}{T}(\langle\xi;\xi\rangle\langle V;V\rangle - \langle\xi;V\rangle^2) + \frac{1}{2}T\langle\xi;\xi\rangle}} \qquad (6)$$

to predict this sound velocity for the systems with any interparticle interaction. In formula (6), $V(\xi)$ is the interparticle potential, $\langle A;B\rangle$ denotes the covariance $\langle AB\rangle - \langle A\rangle\langle B\rangle$ for any two quantities A and B, and $\langle F\rangle$ is the averaged pressure ($\langle F\rangle \equiv 0$ for symmetric potentials). It is thus worthwhile to check whether formula (6) is still valid here. For such a purpose, we numerically measure the velocities of the front peaks for each temperature as shown in $\rho_p(m,t)$ and compare the result with the prediction of formula (6). To gain the theoretical predictions, we insert the ST anharmonic potential [Eq. (2)] into the above formula and calculate the ensemble average of each quantity $\langle A\rangle$ by $\int_{-\infty}^{\infty} Ae^{-V(\xi)/T}\,d\xi / \int_{-\infty}^{\infty} e^{-V(\xi)/T}\,d\xi$.

Figure 7 presents the result of sound velocity with temperatures. As can be seen, the numerical measurements match the predictions quite well, suggesting that, indeed, formula (6) can

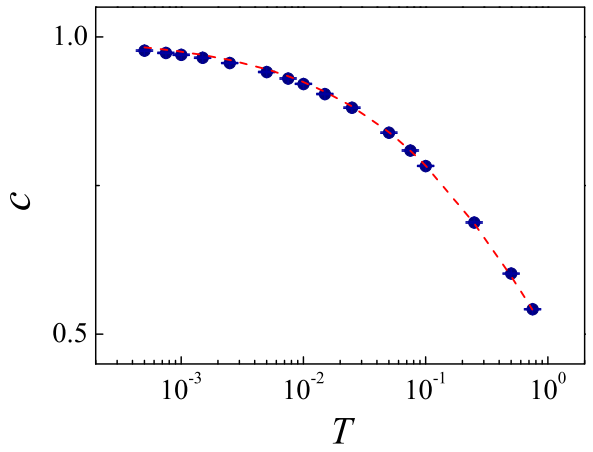

FIG. 7. The sound velocity c vs T, where the dashed line denotes the predictions of formula (6).

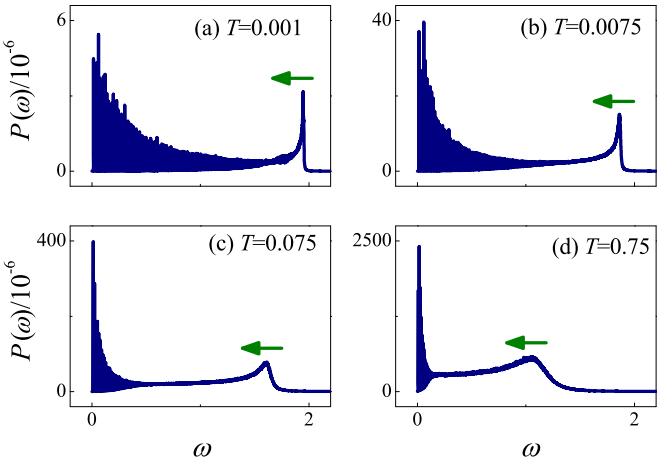

FIG. 8. Phonon spectrum $P(\omega)$ for different temperatures: (a) $T = 0.001$, (b) $T = 0.0075$, (c) $T = 0.075$, (d) $T = 0.75$, respectively.

also be validated to the systems with ST anharmonicity. More importantly, both results indicate the tendency of decrease of sound velocity with temperatures, which is clearly opposite to the results as shown in the FPU-β chains [59]. Thus, this may be a generic feature for systems with ST anharmonicity.

B. Phonons spectrum

Clearly, the decrease of sound velocity cannot be employed to fully understand such temperature variation of heat spread. We next turn to the system's phonon spectrum $P(\omega)$, from which we wish to gain further insights. A quite recent work [41] has suggested that, in addition to the nonballistic behavior of momentum spread, a complete damping of phonons together with phonon softening seem crucial to the observed normal heat transport ($\alpha = 0$, satisfying Fourier's law). Therefore, it would be necessary to explore how both phonon damping and softening would play roles here.

The phonons spectrum $P(\omega)$ are calculated by applying a frequency ω analysis of the particles' velocity $v(t)$ (see the appendix of the review [61]):

$$P(\omega) = \lim_{\tau\to\infty} \frac{1}{\tau} \int_0^\tau v(t) \exp(-i\omega t)\, dt. \qquad (7)$$

To be related to heat spread, this frequency analysis should be done at the corresponding equilibrium states under the same temperatures. For facilitating the computation, here we choose a chain of $L = 200$ particles, then thermalize the chain to the focused temperature by Langevin heat baths [2,3], and finally remove the heat baths and perform a frequency analysis to $v(t)$ following Eq. (7). This should be repeated several times by starting from certain properly assigned initial random states.

Figures 8 and 9 depict the results of the phonon spectrum $P(\omega)$ for different temperatures. Two key points can be revealed from the figures. First, with the increase of T, unlike the systems with HT anharmonicity (hardening phonons), instead, phonons here tend to become "softer" since $P(\omega)$ walks towards the direction of low frequency. This can be captured from the locations of the peaks in the high-frequency parts (see Fig. 8). To clearly characterize such phonons' softening process, one can measure the averaged frequency $\bar{\omega}$ of phonons by defining $\bar{\omega} = \int_0^\infty P(\omega)\omega\, d\omega / \int_0^\infty P(\omega)\, d\omega$. As a complement we plot $\bar{\omega}$ versus T in Fig. 10, from which a monotonous decrease of $\bar{\omega}$ different from the nonmonotonous case as shown in Ref. [41] can be clearly seen. This seems to suggest that only a monotonous phonon softening process is inadequate to induce the normal heat transport. To realize normal transport behavior, very high temperatures or other factors would be necessary to take into account, which needs further efforts of investigations.

Let us finally turn to the results of phonon damping. If they are still called phonons, in their power spectrum at associated frequencies, there should be some oscillations. Indeed, Ref. [41] has suggested that a complete absence of oscillations implies the normal heat transport. With this in mind, one then can employ Fig. 9 to explore the phonon damping process. For such a purpose we use the critical frequency of ω_D below which phonons are damped very weakly to characterize this phonons damping process. As shown in Fig. 9, with the increase of T, the damping first originates from the high-frequency parts [see Figs. 9(a) and 9(b)] and then quickly towards the low

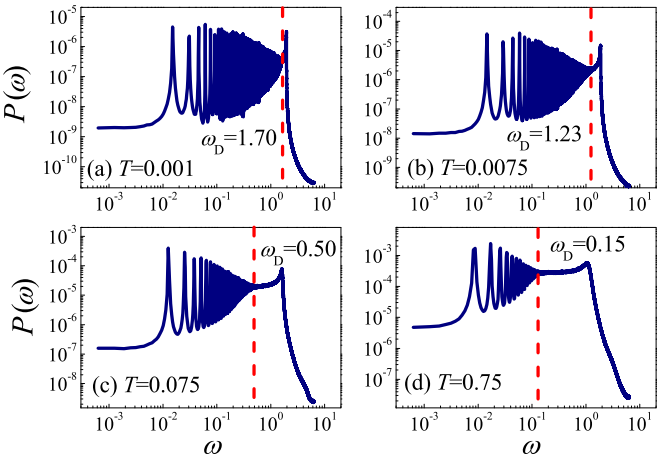

FIG. 9. A log-log plot of Fig. 8, where the dotted lines denote the frequencies ω_D below which phonons are damped very weakly.

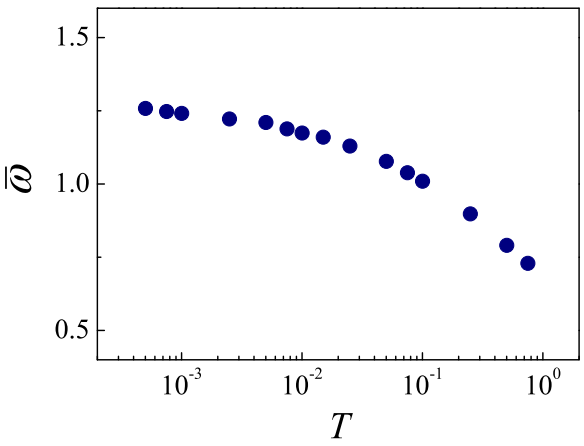

FIG. 10. The averaged frequency $\bar{\omega}$ of phonons shown in $P(\omega)$ vs T.

ones [see Fig. 9(c)]. However, such a quick damping process cannot last forever if one further increases the temperature [see Fig. 9(d)]; eventually, a phonons spectrum very similar to that shown in the FPU-β systems with HT anharmonicity under high nonlinearity [40] can be seen. Based on this numerical evidence, it would be worthwhile to recognize that this incomplete damping process may correspond to the Lévy walk densities observed in $\rho_Q(m,t)$ under high temperatures. It also indicates that both the ST and HT anharmonicity can only lead to an incomplete damping process of phonons; thus, generally, a universal anomalous heat transport with certain temperature-dependent scaling properties could be observed in general nonlinear systems with ST or HT anharmonicity only.

VI. SUMMARY

In summary, we have studied the temperature dependent heat transport behavior in a 1D momentum-conserving system whose interparticle interaction is ST anharmoncity. We have found that by increasing the temperature, including the ST anharmonicity, we can induce some opposite effects to its counterpart FPU-β systems where the interparticle interactions are HT, such as that *monotonously* softening the phonons and decreasing the sound velocity. However, such unusual properties are still inadequate to lead to the normal heat transport. An analysis of phonons spectrum indicates an incomplete damping process of the low-frequency phonons. This property of spectrum is similar to that shown in the FPU-β systems with HT anharmonicity. Our results thus suggest that both ST and HT anharmonicity will eventually lead to a general superdiffusive heat transport behavior, therefore further supporting the conjecture that even strong nonlinearity (here only the deterministic dynamics are considered, which may lead to chaos), either from HT anharmoncity or from ST anharmoncity, is neither a sufficient nor a necessary condition for the validity of Fourier's law [6,7].

ACKNOWLEDGMENTS

This work was supported by the National Natural Science Foundation of China (Grant No. 11575046); the Natural Science Foundation of Fujian Province, China (Grant No. 2017J06002); the Training Plan Fund for Distinguished Young Researchers from Department of Education, Fujian Province, China, and the Qishan Scholar Research Fund of Fuzhou University, China.

[1] J. P. Francoise, G. L. Naber, and T. S. Tsun, *Encyclopedia of Mathematical Physics: Equilibrium Statistical Mechanics; Nonequilibrium Statistical Mechanics* (Science Press, Beijing, 2008).
[2] S. Lepri, R. Livi, and A. Politi, Phys. Rep. **377**, 1 (2003).
[3] A. Dhar, Adv. Phys. **57**, 457 (2008).
[4] S. Lepri, R. Livi, and A. Politi, *Thermal Transport in Low Dimensions*, Lecture Notes in Physics Vol. 921 (Springer, Berlin, 2016).
[5] J. Lebowitz, S. Olla, and G. Stoltz, Final report of workshop *Nonequilibrium statistical mechainics: mathematical understanding and numerical simulation*, http://www.birs.ca/workshops/2012/12w5013/report12w5013.pdf (2013).
[6] G. Casati, J. Ford, F. Vivaldi, and W. M. Visscher, Phys. Rev. Lett. **52**, 1861 (1984).
[7] S. Lepri, R. Livi, and A. Politi, Phys. Rev. Lett. **78**, 1896 (1997).
[8] P. Grassberger, W. Nadler, and L. Yang, Phys. Rev. Lett. **89**, 180601 (2002).
[9] O. Narayan and S. Ramaswamy, Phys. Rev. Lett. **89**, 200601 (2002).
[10] G. Basile, C. Bernardin, and S. Olla, Phys. Rev. Lett. **96**, 204303 (2006).
[11] P. Di Cintio, R. Livi, H. Bufferand, G. Ciraolo, S. Lepri, and M. J. Straka, Phys. Rev. E **92**, 062108 (2015).
[12] T. Mai, A. Dhar, and O. Narayan, Phys. Rev. Lett. **98**, 184301 (2007).
[13] H. van Beijeren, Phys. Rev. Lett. **108**, 180601 (2012).
[14] C. B. Mendl and H. Spohn, Phys. Rev. Lett. **111**, 230601 (2013); H. Spohn, J. Stat. Phys. **154**, 1191 (2014).
[15] V. Zaburdaev, S. Denisov, and J. Klafter, Rev. Mod. Phys. **87**, 483 (2015).
[16] V. Zaburdaev, S. Denisov, and P. Hänggi, Phys. Rev. Lett. **106**, 180601 (2011).
[17] V. Popkov, A. Schadschneider, J. Schmidt, and G. M. Schütz, Proc. Natl. Acad. Sci. USA **112**, 12645 (2015).
[18] S. G. Das, A. Dhar, K. Saito, C. B. Mendl, and H. Spohn, Phys. Rev. E **90**, 012124 (2014).
[19] C. B. Mendl and H. Spohn, Phys. Rev. E **90**, 012147 (2014).
[20] D. Xiong, J. Wang, Y. Zhang, and H. Zhao, Phys. Rev. E **85**, 020102(R) (2012).
[21] D. Xiong, Y. Zhang, and H. Zhao, Phys. Rev. E **88**, 052128 (2013).
[22] D. Xiong, Y. Zhang, and H. Zhao, Phys. Rev. E **90**, 022117 (2014).
[23] G. R. Lee-Dadswell, B. G. Nickel, and C. G. Gray, Phys. Rev. E **72**, 031202 (2005).
[24] G. R. Lee-Dadswell, B. G. Nickel, and C. G. Gray, J. Stat. Phys. **132**, 1 (2008).

[25] G. R. Lee-Dadswell, Phys. Rev. E **91**, 032102 (2015).
[26] P. I. Hurtado and P. L. Garrido, Sci. Rep. **6**, 38823 (2016).
[27] Y. Zhong, Y. Zhang, J. Wang, and H. Zhao, Phys. Rev. E **85**, 060102(R) (2012).
[28] S. Chen, Y. Zhang, J. Wang, and H. Zhao, J. Stat. Mech. (2016) 033205.
[29] A. V. Savin and Y. A. Kosevich, Phys. Rev. E **89**, 032102 (2014).
[30] S. G. Das, A. Dhar, and O. Narayan, J. Stat. Phys. **154**, 204 (2014).
[31] L. Wang, B. Hu, and B. Li, Phys. Rev. E **88**, 052112 (2013).
[32] S. Chen, J. Wang, G. Casati, and G. Benenti, Phys. Rev. E **90**, 032134 (2014).
[33] D. S. Sato, Phys. Rev. E **94**, 012115 (2016).
[34] J. Jiang and H. Zhao, J. Stat. Mech.: Exp. Theor. (2016) 093208.
[35] C. Giardiná, R. Livi, A. Politi, and M. Vassalli, Phys. Rev. Lett. **84**, 2144 (2000).
[36] O. V. Gendelman and A. V. Savin, Phys. Rev. Lett. **84**, 2381 (2000).
[37] S. G. Das and A. Dhar, arXiv:1411.5247v2.
[38] H. Spohn, arXiv:1411.3907v1.
[39] D. Roy, Phys. Rev. E **86**, 041102 (2012).
[40] D. Xiong, Europhys. Lett. **113**, 14002 (2016).
[41] D. Xiong, J. Stat. Mech.: Exp. Theor. (2016) 043208.
[42] H. Zhao, Phys. Rev. Lett. **96**, 140602 (2006).
[43] S. Chen, Y. Zhang, J. Wang, and H. Zhao, Phys. Rev. E **87**, 032153 (2013).
[44] A. Sarmiento, R. Reigada, A. H. Romero, and K. Lindenberg, Phys. Rev. E **60**, 5317 (1999).
[45] R. Reigada, A. H. Romero, A. Sarmiento, and K. Lindenberg, J. Chem. Phys. **111**, 1373 (1999).
[46] A. Sarmiento, A. H. Romero, J. M. Sancho, and K. Lindenberg, J. Chem. Phys. **112**, 10615 (2000).
[47] S. V. Dmitriev, A. P. Chetverikov, and M. G. Velarde, Phys. Status. Solidi B **252**, 1682 (2015).
[48] D. Forster, *Hydrodynamic Fluctuations, Broken Symmetry, and Correlation Functions* (Benjamin, New York, 1975).
[49] J. P. Hansen and I. R. McDonald, *Theory of Simple Liquids*, 3rd ed. (Academic, London, 2006).
[50] D. Xiong and E. Barkai, arXiv:1606.04602v4.
[51] S. Denisov, V. Zaburdaev, and P. Hänggi, Phys. Rev. E **85**, 031148 (2012).
[52] V. Zaburdaev, I. Fouxon, S. Denisov, and E. Barkai, Phys. Rev. Lett. **117**, 270601 (2016).
[53] A. Rebenshtok, S. Denisov, P. Hänggi, and E. Barkai, Phys. Rev. Lett. **112**, 110601 (2014).
[54] A. Rebenshtok, S. Denisov, P. Hänggi, and E. Barkai, Phys. Rev. E **90**, 062135 (2014).
[55] P. Castiglione, A. Mazzino, P. Muratore-Ginanneschi, and A. Vulpiani, Physica D (Amsterdam) **134**, 75 (1999).
[56] S. Denisov, J. Klafter, and M. Urbakh, Phys. Rev. Lett. **91**, 194301 (2003).
[57] B. Li and J. Wang, Phys. Rev. Lett. **91**, 044301 (2003).
[58] In Lévy walks theory there is a generic relation $\alpha = 2 - \gamma$, which is obtained by simultaneously adopting $\alpha = \mu - 1$ and $\mu = 3 - \gamma$, where μ is the time scaling exponent of the displacement's second momentum from the energy fluctuations spreading: $\sigma^2(t) \sim t^{\mu}$; see Ref. [56] for details.
[59] N. Li, B. Li, and S. Flach, Phys. Rev. Lett. **105**, 054102 (2010).
[60] Y. Li, S. Liu, N. Li, P. Hänggi, and B. Li, New J. Phys. **17**, 043064 (2015).
[61] N. Li, J. Ren, L. Wang, G. Zhang, P. Hänggi, and B. Li, Rev. Mod. Phys. **84**, 1045 (2012).